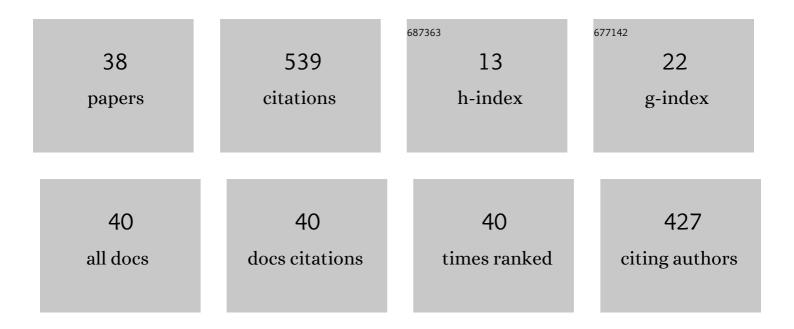
Tilo Zienert

List of Publications by Year in descending order

Source: https://exaly.com/author-pdf/7697581/publications.pdf Version: 2024-02-01



TILO ZIENEDT

#	Article	IF	CITATIONS
1	Interface reactions between liquid iron and alumina–carbon refractory filter materials. Ceramics International, 2015, 41, 2089-2098.	4.8	46
2	Thermodynamic assessment and experiments in the system MgO–Al2O3. Calphad: Computer Coupling of Phase Diagrams and Thermochemistry, 2013, 40, 1-9.	1.6	44
3	Experimental investigation and thermodynamic assessment of the Al-Fe system. Journal of Alloys and Compounds, 2018, 743, 795-811.	5.5	40
4	Reticulated Porous Foam Ceramics with Different Surface Chemistries. Journal of the American Ceramic Society, 2014, 97, 2046-2053.	3.8	39
5	Filtration Efficiency of Functionalized Ceramic Foam Filters for Aluminum Melt Filtration. Metallurgical and Materials Transactions B: Process Metallurgy and Materials Processing Science, 2017, 48, 497-505.	2.1	37
6	Heat capacity of Fe-Al intermetallics: B2-FeAl, FeAl2, Fe2Al5 and Fe4Al13. Journal of Alloys and Compounds, 2017, 725, 848-859.	5.5	33
7	Calculated phase diagrams and thermodynamic properties of the Al 2 O 3 –Fe 2 O 3 –FeO system. Journal of Alloys and Compounds, 2016, 657, 192-214.	5.5	32
8	Wettability of AlSi7Mg alloy on alumina, spinel, mullite and rutile and its influence on the aluminum melt filtration efficiency. Materials and Design, 2018, 150, 75-85.	7.0	27
9	Heat capacity of ÎAlFe (Fe2Al5). Intermetallics, 2016, 77, 14-22.	3.9	20
10	Thermally Induced Formation of Transition Aluminas from Boehmite. Advanced Engineering Materials, 2017, 19, 1700141.	3.5	19
11	Coarse-grained refractory composites based on Nb-Al2O3 and Ta-Al2O3 castables. Ceramics International, 2018, 44, 16809-16818.	4.8	19
12	Phase relations in the ZrO ₂ -Sm ₂ O ₃ -Y ₂ O ₃ -Al ₂ O ₃ -Al ₂ O _{3<!--<br-->system: experimental investigation and thermodynamic modelling. International Journal of Materials Research, 2012, 103, 1469-1487.}	'sub>	18
13	Thermodynamic investigation of the -Al–Fe–Si intermetallic ternary phase: A density-functional theory study. Journal of Alloys and Compounds, 2014, 598, 137-141.	5.5	15
14	<scp>P</scp> hase Relations in the A356 Alloy: Experimental Study and Thermodynamic Calculations. Advanced Engineering Materials, 2013, 15, 1244-1250.	3.5	13
15	Thermodynamics of the Mgâ€Mnâ€O system—modeling and heat capacity measurements. Journal of the American Ceramic Society, 2017, 100, 1661-1672.	3.8	13
16	Mechanical High-Temperature Properties and Damage Behavior of Coarse-Grained Alumina Refractory Metal Composites. Materials, 2019, 12, 3927.	2.9	13
17	Synthesis of Niobium-Alumina Composite Aggregates and Their Application in Coarse-Grained Refractory Ceramic-Metal Castables. Materials, 2021, 14, 6453.	2.9	11
18	Aluminum Melt Filtration with Carbon Bonded Alumina Filters. Materials, 2020, 13, 3962.	2.9	10

TILO ZIENERT

#	Article	IF	CITATIONS
19	Corrosion-Resistant Steel–MgO Composites as Refractory Materials for Molten Aluminum Alloys. Materials, 2020, 13, 4737.	2.9	8
20	Highâ€Temperature Compressive Behavior of Refractory Alumina–Niobium Composite Material. Advanced Engineering Materials, 2022, 24, .	3.5	8
21	Coarseâ€Grained Refractory Composite Castables Based on Alumina and Niobium. Advanced Engineering Materials, 2022, 24, .	3.5	7
22	Comparison of Interfacial Reactions Between Al <scp>S</scp> i7 <scp>M</scp> g and Alumina Filter After Casting and Spark Plasma Sintering**. Advanced Engineering Materials, 2013, 15, 1206-1215.	3.5	6
23	Interface reactions of differently coated carbon-bonded alumina filters with an AZ91 magnesium alloy melt. Ceramics International, 2018, 44, 17415-17424.	4.8	6
24	Prediction of heat capacity for crystalline substances. Calphad: Computer Coupling of Phase Diagrams and Thermochemistry, 2019, 65, 177-193.	1.6	6
25	Effect of MgO Grade in MgO–C Refractories on the Nonâ€metallic Inclusion Population in Alâ€Treated Steel. Steel Research International, 2022, 93, .	1.8	6
26	Formation of different alumina phases and magnesium aluminate spinel during contact of molten AlSi7Mg0.6 alloy with mullite and amorphous silica. Corrosion Science, 2017, 114, 79-87.	6.6	5
27	Characterization of the In Situâ€Formed Oxide Layer at the Steel Melt/Carbonâ€Bonded Alumina Interface. Advanced Engineering Materials, 2020, 22, 1900811.	3.5	5
28	Interface reactions between steel 42CrMo4 and mullite. Journal of the European Ceramic Society, 2015, 35, 1317-1326.	5.7	4
29	Experimental investigation of phase relations and thermodynamic properties in the system ZrO 2 –Eu 2 O 3 –Al 2 O 3. Journal of the European Ceramic Society, 2016, 36, 1455-1468.	5.7	4
30	Metal-Ceramic Beads Based on Niobium and Alumina Produced by Alginate Gelation. Materials, 2021, 14, 5483.	2.9	4
31	Full and Hollow Metal–Ceramic Beads Based on Tantalum and Alumina Produced by Alginate Gelation. Advanced Engineering Materials, 2022, 24, .	3.5	3
32	cp-tools: A Python library for predicting heat capacity of crystalline substances. SoftwareX, 2019, 9, 244-247.	2.6	2
33	Mössbauer spectroscopic and XRD studies of two î-Fe2Al5 intermetallics. Intermetallics, 2021, 135, 107217.	3.9	2
34	Characterization of Sintered Niobium–Alumina Refractory Composite Granules Synthesized by Castable Technology. Advanced Engineering Materials, 2022, 24, .	3.5	2
35	A New Approach for Sintering Simulation of Irregularly Shaped Powder Particles—Part II: Statistical Powder Modeling. Advanced Engineering Materials, 2022, 24, .	3.5	2
36	Low Shrinkage, Coarseâ€Grained Tantalum–Alumina Refractory Composites via Cold Isostatic Pressing. Advanced Engineering Materials, 2022, 24, .	3.5	2

#	Article	IF	CITATIONS
37	Influence of the Wetting Behavior on the Aluminum Melt Filtration. Minerals, Metals and Materials Series, 2019, , 1071-1079.	0.4	1
38	Atomic Force Microscopy Investigation of the In Situâ€Formed Oxide Layer at the Interface of Al 2 O 3 â^'C/Steel Melt in Terms of Adhesion Force and Roughness in a Model System. Advanced Engineering Materials, 0, , 2100634.	3.5	0